
Self-Assembly of 4-sided Fractals in the Two-handed Tile Assembly Model

Jacob Hendricks · Joseph Opseth

Abstract We consider the self-assembly of fractals in one of the most well-studied models of tile based self-assembling systems known as the Two-handed Tile Assembly Model (2HAM). In particular, we focus our attention on a class of fractals called discrete self-similar fractals (a class of fractals that includes the discrete Sierpiński carpet). We present a 2HAM system that finitely self-assembles the discrete Sierpiński carpet with scale factor 1. Moreover, the 2HAM system that we give lends itself to being generalized and we describe how this system can be modified to obtain a 2HAM system that finitely self-assembles one of any fractal from an infinite set of fractals which we call *4-sided fractals*. The 2HAM systems we give in this paper are the first examples of systems that finitely self-assemble discrete self-similar fractals at scale factor 1 in a purely growth model of self-assembly. Finally, we show that there exists a *3-sided fractal* (which is not a tree fractal) that cannot be finitely self-assembled by any 2HAM system.

1 Introduction

The study of fractals has both a mathematical and a practical basis, as patterns similar to these recursively self-similar patterns occur in nature in the form of circulatory systems and branch patterns. Evidently many fractals found in nature are the result of a process where a simple set of rules dictating how individual basic components (such as individual molecules) interact to yield

larger complexes with recursive self-similar structure. One approach to understanding this process is to model such a process with artificial self-assembling systems.

One of the first and also one of the most studied mathematical models of self-assembling systems is Winfree’s abstract Tile Assembly Model (aTAM) [43] where individual autonomous components are represented as tiles with glues on their edges. The aTAM was intended to model DNA tile self-assembly, where tiles are implemented using DNA molecules. In the context of DNA tile self-assembly, there have been two main reasons for considering the self-assembly of fractals. First, in [17] and [40], DNA-based tiles are used to self-assemble the Sierpiński triangle, showing the potential for DNA tile self-assembly to be used for the controlled formation of complex nanoscale structures. Second, there are many proposed theoretical models (and generalizations of these models) of DNA tile self-assembly (see [1, 6, 9, 12, 14, 24, 27, 35, 43] for some examples). While mathematical notions of simulation relations between systems in such models continue to further elucidate how these various models relate [3, 10, 13, 22, 33, 34], many “benchmark” problems have also been introduced. These benchmarks include the efficient self-assembly of squares and/or general shapes [11, 37, 41, 42], the capacity to perform universal computation [7, 15, 16, 18, 21, 35, 37], and the self-assembly of fractals [2, 20, 28, 29, 32, 38, 39]. In addition to providing a way of benchmarking models of self-assembly, studying the self-assembly of fractals has the potential to lead to new techniques for the design self-assembling systems.

When considering the self-assembly of discrete self-similar fractals (dssf’s) such as the Sierpiński triangle one can consider either “strict” self-assembly, wherein a shape is made by placing tiles only within the domain of the shape, or “weak” self-assembly where a pattern representing the shape forms as part of a complex of

Department of Computer Science and Information Systems,
University of Wisconsin - River Falls, jacob.hendricks@uwrf.edu

Department of Mathematics, University of Wisconsin - River
Falls, joseph.opseth@my.uwrf.edu

tiles that contains specially labeled tiles corresponding to points in the shape and possibly additional tiles not corresponding to points of the shape. Previous work (including [2, 28, 29, 32, 38, 39]) has shown the difficulty of strict self-assembly of dssf's in the aTAM as no non-trivial dssf has been shown to self-assemble in the strict sense. In fact, the Sierpiński triangle is known to be impossible to self-assemble in the aTAM [30]; though it is possible to design systems which “approximate” the strict self-assembly of fractals [30, 32, 38]. Interestingly, it is unknown whether there exists a dssf which strictly self-assembles in the aTAM. This includes the Sierpiński carpet dssf. In this paper, we consider 2HAM systems which “finitely” self-assemble dssf's. Finite self-assembly was defined in [3] to study 2HAM systems that self-assemble infinite shapes (e.g. dssf's). Intuitively, a shape S , finitely self-assembles in a tile assembly system if any finite producible assembly of the system can always continue to self-assemble into the shape S and the shape of any finite producible assembly is a sub-shape of S . See [3, 5, 19] for results which use the definition of finite self-assembly.

While the aTAM models single tile attachment at a time (or step in the self-assembly process), a more generalized model and another of the most studied models of self-assembly called the 2-Handed Assembly Model [6] (2HAM, a.k.a. Hierarchical Assembly Model) allows pairs of large assemblies to bind together. Given the hierarchical nature of the self-assembly process modeled by the 2HAM, we consider employing this process to finitely self-assemble dssf's. In [5] it is shown that the Sierpiński carpet finitely self-assembles in the 2HAM at temperature 2, but with scale factor 3. That is, instead of finitely self-assembling a structure with tiles corresponding to the points of the Sierpiński carpet, the structure that self-assembles contains a 3 by 3 block of tiles that corresponds to a single point of the Sierpiński carpet. Here we show that not only does the Sierpiński carpet finitely self-assemble with scale factor 1, but an infinite class of fractals, which we call the 4-sided fractals, finitely self-assembles at temperature 2 in the 2HAM with scale factor 1. Intuitively, 4-sided fractals are fractals that have a generator (the set of points in the first stage of the fractal) such that the generator is connected and consists of a rectangle of points “on the boundary” of the generator as well as points “inside” this rectangle. In other words, a 4-sided fractal is a fractal with a generator that contains all 4 sides and one can define 0, 1, 2, and 3-sided fractals analogously. (Definitions are given in Section 2.) Moreover, we show that there exists a 3-sided fractal that cannot be finitely self-assembled by any 2HAM system at any temperature.

Theorem 1 implies that one of the most well-known dssf's (the Sierpiński carpet) finitely self-assembles in one of the simplest and most studied models of self-assembly, the 2HAM. It should be noted that in [20] it is shown that *any* dssf can finitely self-assemble in the Signal-passing Tile Assembly Model (STAM) where tiles can change state and even disassociate from an existing assembly, “breaking” an assembly into two disconnected assemblies. That is, given any dssf, there is a STAM system that finitely self-assembles this fractal. Additionally, in [20] it is shown that a large class of fractals finitely self-assembles in the STAM even with temperature restricted to 1. In a model similar to the STAM, the Active Tile Assembly Model [25], infinite, self-similar substitution tiling patterns which fill the plane have been shown to assemble [26]. This may be considered a testament to the power of active tiles. Here we show that it is still possible to finitely self-assemble an infinite class of fractals in the 2HAM even though tiles are not active and disassociation is not allowed.

2 Preliminaries

Here we provide informal descriptions of the 2HAM. For more details see [3, 6, 36]. Definitions and notation in Section 2.1 are based on definitions from [3–5]. Similar definitions and notation for the 2HAM can also be found in [10, 23, 31]. We restate the definitions in the context of this paper for the sake of completeness and convenience. Likewise, in Section 2.2, we also give the definition of discrete self-similar fractals similar to the definitions found in [2] and [20].

2.1 Informal description of the 2HAM

Let $U_2 = \{(0, 1), (0, -1), (1, 0), (-1, 0)\}$ be the set of all unit vectors in \mathbb{Z}^2 . A *grid graph* is a graph $G = (V, E)$ such that $V \subseteq \mathbb{Z}^2$, and for any edge $\{\vec{a}, \vec{b}\} \in E$, $\vec{a} - \vec{b} \in U_2$.

2.1.1 Tile types, tiles, and supertiles

A *tile type* is a unit square with 4 well defined sides that each correspond to a vector in U_2 such that each side of the square has an associated *glue*. A glue is defined by a *label* and a *strength*. A glue label is a string of symbols over some fixed alphabet, and a glue strength is a non-negative integer. Moreover, a tile type has an associated string of symbols over some fixed alphabet called a *label*. A *positioned tile* is a pair consisting of a tile type and a point in \mathbb{Z}^2 called a *tile location*. A *tile* is the set of all translations in \mathbb{Z}^2 of a positioned tile. We

refer to the side of a tile type (or tile) corresponding to $(0, 1)$, $(0, -1)$, $(1, 0)$, or $(-1, 0)$ as the north, south, east, or west edge of the tile type (or tile) respectively.

Let T be a finite set of tile types. A *positioned supertile over T* is a set of positioned tiles with tile types in T such that the positioned tiles have distinct tile locations. For a positioned supertile A over T , we let $|A|$ denote the cardinality of A . A *supertile over T* is the set of all translations of a positioned supertile over T . For a positioned supertile A , note that cardinality is invariant under translation. Therefore, for a supertile α over T , we let $|\alpha|$ denote the cardinality of any positioned supertile in α and note that this is well-defined. When T is clear from context, we will shorten the phrase “supertile over T ” to simply “supertile”. For two adjacent tiles t_1 and t_2 in a positioned supertile over T and s in \mathbb{N} , we say that t_1 and t_2 *interact with strength s* if the glues on their abutting sides are equal¹ and these glues have non-zero strengths equal to s .

Let A be a positioned supertile over T . The *binding graph of A* is the weighted undirected grid graph $G = (V, E)$ such that 1) V is the set of all tile locations of tiles in A , and 2) E is the set of all unordered pairs of vertices v_1 and v_2 in $V \times V$ with weight $w \in \mathbb{N}$ such that the two tiles in A with tile locations equal to v_1 and v_2 interact with strength w . Note that a binding graph is a grid graph. For a non-negative integer τ , A is τ -*stable* if for every cut C of the binding graph of A , the sum of the weights of the edges in the cut-set of C is greater than or equal to τ . A supertile α over T is τ -stable if it contains a positioned supertile over T that is τ -stable. Note that if A is τ -stable, then any translation of A is τ -stable. Therefore, the notion of τ -stable for supertiles is well-defined.

Let A , B , and C be positioned supertiles over T such that A and B are τ -stable. We say that A and B are τ -*combinable into C* if $C = A \cup B$ and C is τ -stable. Moreover, let α , β , and γ be supertiles over T such that α and β are τ -stable. α and β are τ -*combinable into γ* if there exists A in α , B in β , and C in γ such that A and B are τ -combinable into C . Note that if α and β are τ -combinable into γ , then γ is τ -stable. We also define the *subassembly* relation between two supertiles as follows. For supertiles α and β , α is a subassembly of β provided that there exist positioned supertiles A in α and B in β such that $A \subseteq B$.

2.1.2 Tile assembly systems and assembly sequences

A *tile assembly system* (TAS) in the 2HAM is defined to be an ordered pair $\mathcal{T} = (T, \tau)$ such that T is a finite set of tile types, and τ is a positive integer which we

¹ glue labels are equal and glue strengths are equal

call the *temperature* of \mathcal{T} . Let $\mathcal{T} = (T, \tau)$ be a TAS. A *state S* is a multiset of τ -stable supertiles over T such that the multiplicity of any supertile in S is in $\mathbb{N} \cup \{\infty\}$. Let S_0 and S_1 be states. S_0 *transitions* to S_1 at temperature τ if 1) there exists a supertile γ such that $S_1 = S_0 \cup \{\gamma\}$, and 2) there exists α and β in S_0 such that α and β are τ -combinable into γ .

Let k be in $\mathbb{N} \cup \{\infty\}$. A *state sequence* of \mathcal{T} is a sequence of states $\mathbf{S} = \langle S_i \rangle_{i=0}^k$ such that for all i , S_i transitions to S_{i+1} . A state sequence is called *nascent* if S_0 is the multiset consisting of infinitely copies of tiles, one tile for each tile type in T . For a producible supertile α , an *assembly sequence* for α is a sequence of supertiles $\boldsymbol{\alpha} = \langle \alpha_i \rangle_{i=0}^k$ such that there exists a state sequence $\mathbf{S} = \langle S_i \rangle_{i=0}^k$ such that for all $i < k$, $\alpha_i \in S_i$ and there exists a supertile $\beta_i \in S_i$ such that α_i and β_i are τ -combinable into α_{i+1} . Such an assembly sequence is called *nascent* if \mathbf{S} is nascent. The *result* of an assembly sequence $\boldsymbol{\alpha} = \langle \alpha_i \rangle_{i=0}^k$ is the unique supertile ρ such that there exists $R \in \rho$ and $A_i \in \alpha_i$ such that $R = \cup_{0 \leq i < k} A_i$, and for each i such that $0 \leq i < k$, α_i is a subassembly of ρ .

2.1.3 Producing supertiles and shapes

Given a TAS $\mathcal{T} = (T, \tau)$, a supertile is *producible* if it is the result of a nascent assembly sequence. A producible supertile α is *terminal* if for any producible supertile β there does not exist a τ -stable supertile γ such that α and β are τ -combinable into γ . We refer to the set of producible supertiles for \mathcal{T} as $\mathcal{A}[\mathcal{T}]$ and the set of terminal supertiles for \mathcal{T} as $\mathcal{A}_{\square}[\mathcal{T}]$.

We refer to a set of points in \mathbb{Z}^2 as a *shape*. For a shape X , a supertile α *has shape X* if there exists a positioned supertile A in α such that the set of tile locations of positioned tiles in A is equal to X . Given a TAS $\mathcal{T} = (T, \tau)$, for an infinite shape $X \subseteq \mathbb{Z}^2$, we say that \mathcal{T} *finitely self-assembles X* if for every finite producible supertile α of \mathcal{T} , α has the shape of a subset of points in X , and there exist an assembly sequence $\boldsymbol{\alpha} = \langle \alpha_i \rangle_{i=0}^{\infty}$ such that $\alpha_0 = \alpha$ and the result of $\boldsymbol{\alpha}$ has shape X . In this paper we consider finite self-assembly of dssf's.

2.2 Discrete Self-Similar Fractals

In order to state the main theorem, we need to provide a few definitions. The definition of a discrete self-similar fractals and some of the notation used here also appears in [2, 20, 38]. First we introduce some notation.

Given $V \subseteq \mathbb{Z}^2$, the *full grid graph* of V is the undirected graph $G_V^f = (V, E)$, such that for all $\mathbf{x}, \mathbf{y} \in V$, $\{\mathbf{x}, \mathbf{y}\} \in E$ iff $\|\mathbf{x} - \mathbf{y}\| = 1$.

Let \mathbb{N}_g denote the subset $\{0, \dots, g-1\}$ of \mathbb{N} , and let $\mathbb{N}_g^2 = \mathbb{N}_g \times \mathbb{N}_g$. For $g \in \mathbb{N}$ and $G \subseteq \mathbb{N}_g^2$, let l_G, r_G, b_G , and t_G denote the integers: $l_G = \min_{(x,y) \in G} x$, $r_G = \max_{(x,y) \in G} x$, $b_G = \min_{(x,y) \in G} y$, and $t_G = \max_{(x,y) \in G} y$. Moreover, let $w_G = r_G - l_G + 1$ and $h_G = t_G - b_G + 1$ denote the *width* and *height* of G respectively. Finally, let $L_G = \{(l_G, y) \mid b_G \leq y \leq t_G\}$, $R_G = \{(r_G, y) \mid b_G \leq y \leq t_G\}$, $T_G = \{(x, t_G) \mid l_G \leq x \leq r_G\}$, and $B_G = \{(x, b_G) \mid l_G \leq x \leq r_G\}$. In other words, L_G, R_G, T_G , and B_G are the sets of points belonging to left, right, top, and bottom line segments of a “bounding box” of G . Finally, if A and B are subsets of \mathbb{N}^2 and $(x, y) \in \mathbb{N}^2$, then $A + (x, y)B = \{(x_a, y_a) + (x \cdot x_b, y \cdot y_b) \mid (x_a, y_a) \in A \text{ and } (x_b, y_b) \in B\}$. First we give the definition of a discrete self-similar fractal.

Definition 1 Let $\mathbf{X} \subset \mathbb{N}^2$. We say that \mathbf{X} is a *discrete self-similar fractal* (or *dssf* for short), if there is a set $\{(0, 0)\} \subset G \subset \mathbb{N}_g^2$ with at least one point in every row and column, such that

1. the full grid-graph of G is connected,
2. $w_G > 1$ and $h_G > 1$,
3. $G \subsetneq \mathbb{N}_{w_G} \times \mathbb{N}_{h_G}$, and
4. $\mathbf{X} = \cup_{i=1}^{\infty} X_i$, where X^i , the i^{th} stage of \mathbf{X} , is defined by $X^1 = G$ and $X^{i+1} = X^i + (w_G^i, h_G^i)G$.

Moreover, we say that G is the *generator* of \mathbf{X} .

A connected discrete self-similar fractal is one in which every component is connected in every stage, i.e. there is only one connected component in the grid graph formed by the points of the shape.

Definition 2 Let $n \in \{0, 1, 2, 3, 4\}$, $1 < g \in \mathbb{N}$ and $\mathbf{X} \subset \mathbb{N}^2$. We say that \mathbf{X} is a *n-sided fractal* if \mathbf{X} is a discrete self-similar fractal with generator G such that:

1. the full grid graph of G is connected,
2. $S \cap G = S$ for at least n distinct sets S in $\{L_G, R_G, T_G, B_G\}$.

Intuitively, the second condition in Definition 2 is saying that the fractal generator contains all points of at least n of the left, right, top, and bottom line segments of a “bounding box” of G . In particular, the generator of a 4-sided fractal contains all of the points along the left, right, top, and bottom “sides” of the fractal generator. Finally, for a fractal \mathbf{X} with generator G , an enumeration of the points in a generator $G = \{\mathbf{v}_i\}_{i=1}^{|G|}$, and $j \in \mathbb{N}$, the stages of \mathbf{X} are $X^1 = G$ and $X^{j+1} = X^j + (w_G^j, h_G^j)G$. For $i \in \mathbb{N}$ such that $1 \leq i \leq |G|$, we call the points of the $j+1$ stage given by $X_j + (w_G^j, h_G^j)\mathbf{v}_i$ the j^{th} stage at position i . For dssf \mathbf{X} and $i \in \mathbb{N}$ such that $i \geq 1$, we let X^i denote the i^{th} stage of \mathbf{X} .

3 Self-assembly of Four Sided Fractals

In this section we show how to finitely self-assemble the class of 4-sided discrete self-similar fractals in the 2HAM with scale factor of 1 (i.e. no scaling is required). The most well-known example of a 4-sided fractal is the Sierpiński carpet.

Theorem 1 Let \mathbf{X} be a 4-sided fractal. Then, there exists a 2HAM $TAS \mathcal{T}_{\mathbf{X}} = (T, 2)$ that finitely self-assembles \mathbf{X} . Moreover, if G is the generator for \mathbf{X} and $|G| = g$, $|T|$ is $O(g^3)$.

We build intuition for a construction showing Theorem 1 by showing that the Sierpiński carpet finitely self-assembles in the 2HAM at scale factor 1. We then describe the modifications needed to extend the construction for the Sierpiński carpet to all 4-sided fractals.

3.1 The Sierpiński carpet construction overview

The Sierpiński carpet dssf is the dssf with generator $G = \{(0, 2), (1, 2), (2, 2), (0, 1), (1, 2), (0, 0), (1, 0), (2, 0)\}$. Figure 1a depicts this generator, while Figures 1b and 1c depict the second and third stages of the dssf respectively. We denote the carpet dssf by \mathbf{S} and for $i \in \mathbb{N}$, we denote the i^{th} stage of \mathbf{S} as S^i . We enumerate the points of S^1 as depicted in Figure 1a and use this enumeration to reference the positions of some substage within a subsequent stage of the carpet.

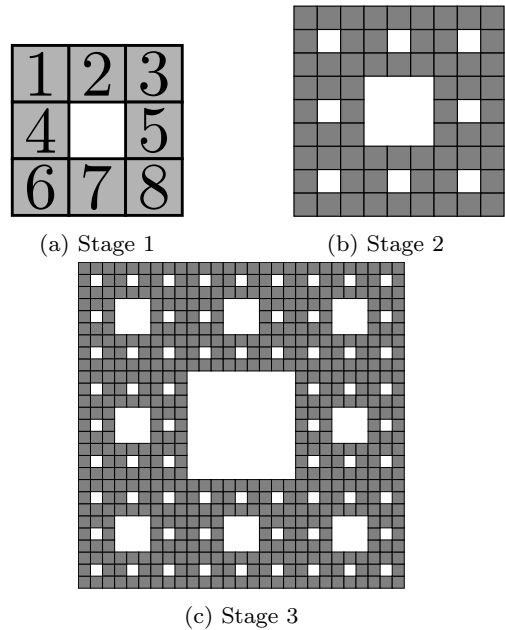


Fig. 1: Three stages of the Sierpiński carpet

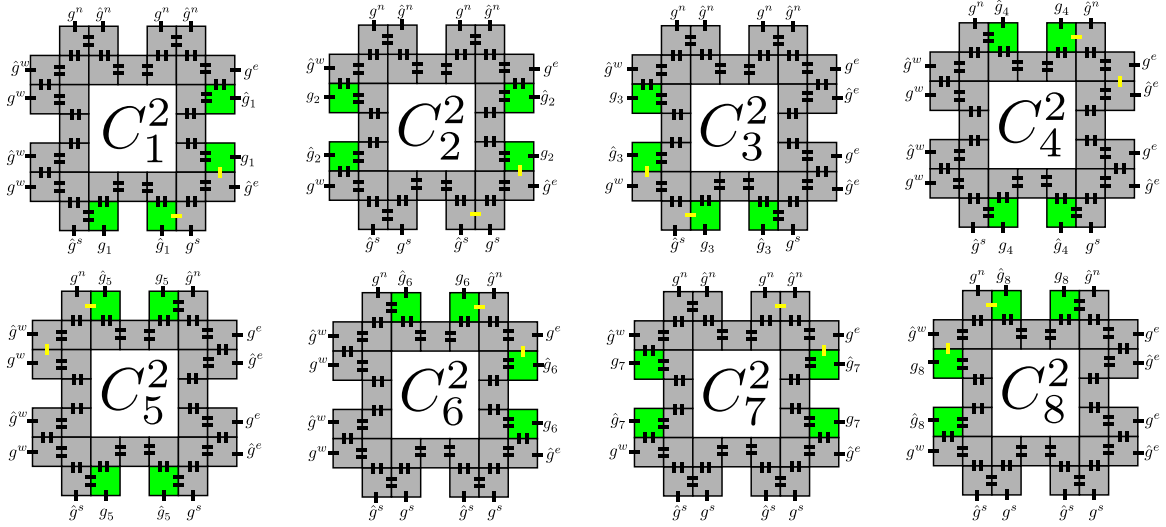


Fig. 2: The tiles that self-assemble a stage 2 supertile C_i^2 . The unlabelled strength 1 and 2 black and yellow glues shown on edges of two adjacent tiles in each of the 8 supertiles are defined to have matching type. Moreover, these glues do not match any other glues of other tile types in T . In other words, tiles types have been “hard-coded” so that each of these 8 supertiles self-assembles.

We now describe the tile set, T , that is used to finitely self-assemble \mathcal{S} in the 2HAM at temperature $\tau = 2$ at scale factor 1.

3.1.1 The Sierpiński carpet tile set

To define the tile set T , we begin by distinguishing between two classes of tile types called **grout** tile types and **initializer** tile types. We say **grout** (respectively **initializer**) tiles or supertiles when referring to tiles or supertiles consisting only of tiles with **grout** (respectively **initializer**) tile types. At a high-level, **initializer** tiles self-assemble into supertiles corresponding to \mathcal{S} at stage 2, and **grout** tile types self-assemble into supertiles which facilitate the self-assembly of each consecutive stage of \mathcal{S} starting from the stage 2 supertiles self-assembled by **initializer** tile types. We first describe **initializer** tile types.

3.1.1.1 Self-assembly of stage 2 by initializer tile types

The **initializer** tiles self-assemble to form 8 different supertiles, the domains of which are contained in a portion of S^2 . See Figure 2 for a depiction of these 8 supertiles. We denote these 8 supertiles by C_i^2 for $1 \leq i \leq 8$. For each i , we define 32 unique tile types of T that self-assemble the supertile C_i^2 corresponding to a portion of S^2 that will be in the i^{th} position of a supertile corresponding to a portion of S^3 (this portion is depicted in Figure 10). The main idea is that tiles that self-assemble C_i^2 have been “hard-coded” (i.e. for any

glue on the edge of some tile, there exists a single matching glue on another tile) to ensure that for each i , C_i^2 self-assembles. Moreover, tile types are defined so that all tiles of C_i^2 self-assemble before C_i^2 can be contained in a strictly larger supertile. In other words, referring to Figure 9, the gray and green tiles self-assemble supertiles consisting C_i^2 before any of the the aqua tiles can attach. To see this, note the presence of the yellow glues in the supertiles shown in Figure 2. These yellow glues restrict the assembly sequences for each supertile at temperature 2. In particular, the final step in the assembly sequence of C_1^2 is the binding event between a supertile of size 3 and a supertile of size 29 via two yellow glues. Therefore, C_1^2 is completely self-assembled exactly when glues g_1 and g^s are exposed by edges of tiles of C_1^2 , and only after these glues are present can a supertile (called a **start-gadget** and described in more detail in Section 3.1.1.2) shown in Figure 3a bind, leading to a supertile strictly containing C_1^2 as a subassembly.

Referring to Figure 2, note that for each i , C_i^2 supertiles may expose glues of type g^d or \hat{g}^d for d either n , s , e , or w , as well as possibly g_k or \hat{g}_k for $1 \leq k \leq 8$. These glues allow **grout** supertiles to cooperatively bind and the glues labeled g_k and \hat{g}_k indicate where special **grout** supertiles should bind, hence they are called **indicator** glues. Tiles containing an edge with an indicator glue are depicted in green in Figure 2.

The self-assembly of supertiles corresponding to stage 3 of the Sierpiński carpet will require **grout** tile types. These tile types are described in the next section. We first describe how **grout** tile types facilitate the self-

assembly of supertiles corresponding to stage 3 of the carpet and then describe how these same **groat** tile types facilitate the self-assembly of supertiles corresponding to any stage, s say, by binding to supertiles corresponding to stage $s - 1$.

3.1.1.2 groat tile types and stage 3 carpet assembly

Figures 3-8 describe **groat** supertiles that bind to C_1^2 or C_2^2 . For a depiction of the **groat** supertiles that bind to C_i^2 for $3 \leq i \leq 8$, see Section A. We describe the **groat** supertiles that attach to C_1^2 and C_2^2 , and note that the **groat** supertiles that attach to C_i^2 for $3 \leq i \leq 8$ are similar.

For each i , there are 8 different classes of **groat** tile types which we enumerate with 1 through 8 that can bind to supertile C_i^2 . In other words, for each supertile Figures 3-8, tile types for **groat** tiles are defined so that eight different versions of each of **groat** supertiles, corresponding to eight **groat** classes, self-assemble. In each figure, $j \in \mathbb{N}$ is such that $1 \leq j \leq 8$, and tiles of supertiles belong to **groat** class j . Depending on the value of j , for $k \in \mathbb{N}$ such that $1 \leq k \leq 8$, the glues $h_{k,j}$, $\hat{h}_{k,j}$, $h_{1,j}^*$, and $\hat{h}_{1,j}^*$ are defined to either have strength 1 or 0. Table 1 describes glue strengths for these glues for each j . In addition, for $p \in \{2, 4, 5, 7\}$, glues with labels $\hat{g}_{p,j}$ and $\bar{g}_{p,j}$ are defined in Table 2.

The **groat** tiles are hard-coded to self-assemble **groat** supertiles such that only **groat** tiles belonging to the same class can bind. Moreover, two distinct **groat** supertiles have matching glues iff the tiles of these supertiles have types belonging to the same **groat** class. That is, for each i , **groat** supertiles with tiles of any one, and only one, of the 8 **groat** classes can bind to some C_i^2 . For example, the **groat** supertiles that bind to some C_i^2 before any other **groat** supertiles are called **start-gadget** supertiles. See Figure 3 for examples of **start-gadget** supertiles.

j	glues with strength 0
1	$h_{5,j}, \hat{h}_{7,j}$
2	$h_{5,j}, \hat{h}_{7,j}$
3	$\hat{h}_{4,j}, \hat{h}_{6,j}$
4	$h_{2,j}, \hat{h}_{3,j}$
5	$h_{1,j}, \hat{h}_{1,j}^*$
6	$h_{2,j}, \hat{h}_{3,j}$
7	$h_{2,j}, \hat{h}_{3,j}$
8	$h_{1,j}, \hat{h}_{1,j}^*$

Table 1: For $j \in \mathbb{N}$ such that $1 \leq j \leq 8$, this table lists those glues defined to have strength 0. For all $k \in \mathbb{N}$ such that $1 \leq k \leq 8$, $h_{k,j}$, $\hat{h}_{k,j}$, $h_{1,j}^*$, and $\hat{h}_{1,j}^*$ not listed in a row for a fixed value j are defined to have strength 1.

j	$\hat{g}_{2,j}$	$\bar{g}_{2,j}$	$\hat{g}_{4,j}$	$\bar{g}_{4,j}$	$\hat{g}_{5,j}$	$\bar{g}_{5,j}$	$\hat{g}_{7,j}$	$\bar{g}_{7,j}$
1	\hat{g}^n	g^n	\hat{g}^w	g^w	\hat{g}_1	g_1	g_1	\hat{g}_1
2	\hat{g}^n	g^n	\hat{g}_2	g_2	g_2	\hat{g}_2	g^s	\hat{g}^s
3	\hat{g}^n	g^n	\hat{g}_3	g_3	g^e	\hat{g}^e	g_3	\hat{g}_3
4	\hat{g}_4	g_4	\hat{g}^w	g^w	g^e	\hat{g}^e	g_4	\hat{g}_4
5	\hat{g}_5	g_5	\hat{g}^w	g^w	g^e	\hat{g}^e	g_5	\hat{g}_5
6	\hat{g}_6	g_6	\hat{g}^w	g^w	g_6	\hat{g}_6	g^s	\hat{g}^s
7	\hat{g}^n	g^n	\hat{g}_7	g_7	g_7	\hat{g}_7	g^s	\hat{g}^s
8	\hat{g}_8	g_8	\hat{g}_8	g_8	g^e	\hat{g}^e	g^s	\hat{g}^s

Table 2: For $j \in \mathbb{N}$ such that $1 \leq j \leq 8$, this table gives glue definitions. For example, when $j = 1$, $\hat{g}_{2,j} = \hat{g}^n$. All glues in this table are also defined to have strength 1.

For i between 1 and 8 (inclusive), after supertiles C_i^2 self-assemble, **groat** tiles attach to these supertiles to form supertiles which expose glues that allow them to bind to each other to self-assemble a supertile corresponding to stage 3 of the Sierpiński carpet. Figure 9 shows each supertile C_i^2 for $1 \leq i \leq 8$ along with **groat** supertiles with **groat** class j attached. Figure 10 gives a depiction of the portion of S^3 that self-assembles; **groat** supertiles in this figure are depicted in aqua.

Starting from some supertile C_i^2 , initial growth of **groat** tiles begins when a **start-gadget** cooperatively binds to some C_i^2 via pairs of glues exposed by each supertile C_i^2 . Figure 3a depicts such a supertile that binds to a C_1^2 supertile when the glues g_1 and g^s cooperatively bind to the matching glues of C_1^2 . One can observe that the glues of **groat** supertiles have been defined so that binding of **groat** supertiles to C_i^2 for $1 \leq i \leq 8$ always begins with the attachment of a **start-gadget** supertile.

Glues of **groat** tiles have also been defined so that after a **start-gadget** binds to C_i^2 for some i , **groat** supertiles cooperatively bind one at a time and partially surround the supertile C_i^2 as in Figure 9. We refer to the **groat** supertiles other than **start-gadget** supertiles that cooperatively bind to C_i^2 as **crawler** supertiles. Figures 4 and 5. depict **crawler** supertiles that bind to C_1^2 , and Figures 6, 7, and 8 depict **crawler** supertiles that bind to C_2^2 .

A **groat** tile that binds to an indicator glue (for $1 \leq k \leq 8$, glues with label g_k or \hat{g}_k in Figure 2) of a south edge of a tile belonging to C_i^2 (respectively north, east, or west) will have a glue on its south (respectively north, east, or west) edge. The strength of such a glue is either 0 or 1 as given in Table 1. The type of glue and whether or not a **groat** tile exposes such a glue depends on the class of the **groat** supertiles that attach to some C_i^2 . We call these glues exposed on an edge of a **groat** tile **stage-binding** glues. In Figures 3 through 8 and 9, **stage-binding** glues are $h_{1,j}^*$, $\hat{h}_{1,j}^*$, or $h_{k,j}$, $\hat{h}_{k,j}$ for $1 \leq k \leq 8$. Strength-1 **stage-binding**

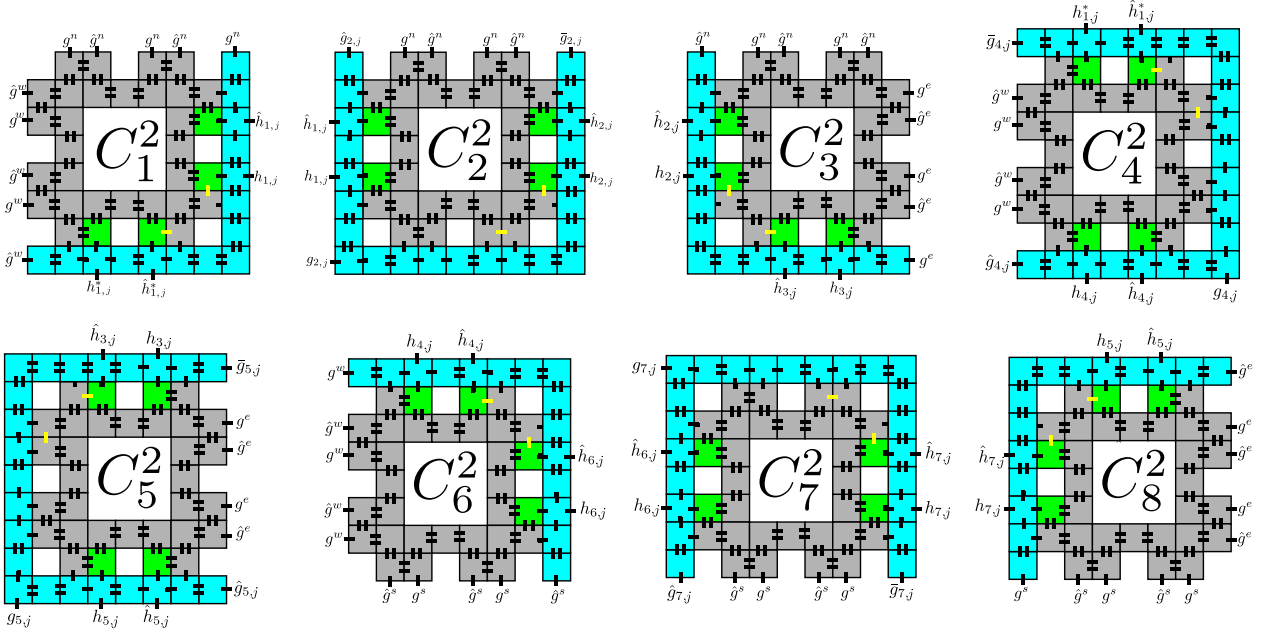


Fig. 9: Supertiles $C_{(i,j)}^2$ for $1 \leq i \leq 8$ and some j such that $1 \leq j \leq 8$. Depending on j , certain glues will have strength of 0 as described in Table 1 though they are shown here as strength-1 glues.

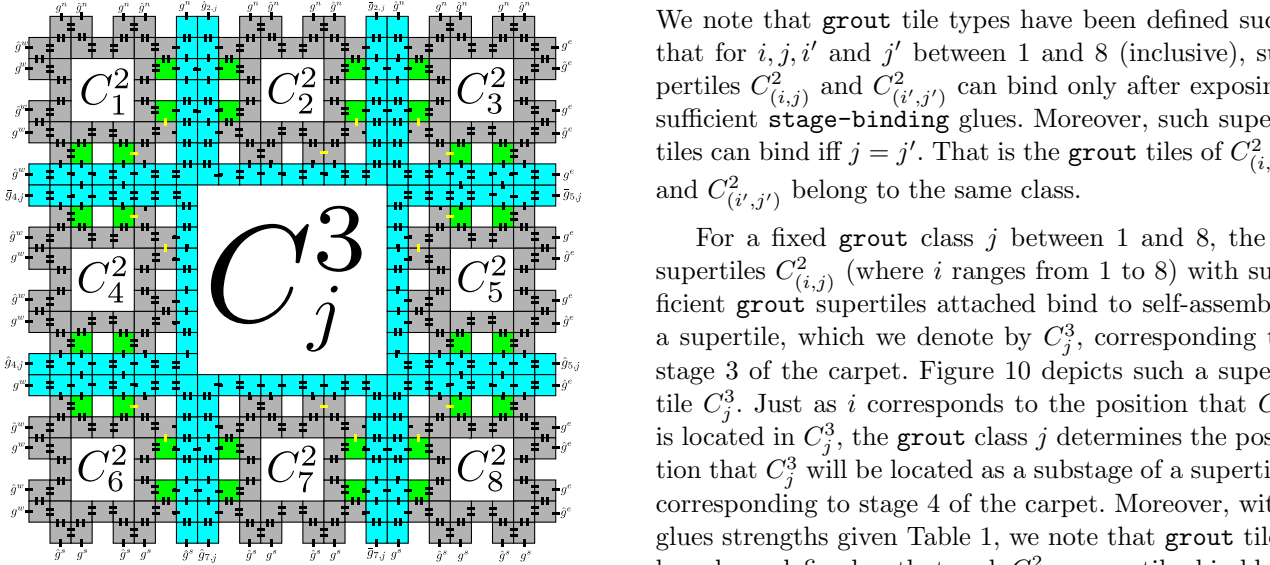


Fig. 10: A depiction of C_j^3 . Note that for $p \in \{2, 4, 5, 7\}$ the glues $\hat{g}_{p,j}$ and $\bar{g}_{p,j}$ shown here are defined in Table 2.

glues exposed by grout supertiles bound to C_i^2 supertiles bind to allow for the self-assembly of a supertile that corresponds to the third stage of the carpet.

Now let $C_{(i,j)}^2$ denote any supertile consisting only of tiles of C_i^2 and grout tiles of class j . Figure 9 depicts such supertiles. The supertiles depicted in Figure 9 are such that no other grout supertiles can bind to a given C_i^2 and have been depicted this way to show all of the glues exposed after grout supertiles bind to each C_i^2 .

We note that grout tile types have been defined such that for i, j, i' and j' between 1 and 8 (inclusive), supertiles $C_{(i,j)}^2$ and $C_{(i',j')}^2$ can bind only after exposing sufficient stage-binding glues. Moreover, such supertiles can bind iff $j = j'$. That is the grout tiles of $C_{(i,j)}^2$ and $C_{(i',j')}^2$ belong to the same class.

For a fixed grout class j between 1 and 8, the 8 supertiles $C_{(i,j)}^2$ (where i ranges from 1 to 8) with sufficient grout supertiles attached bind to self-assemble a supertile, which we denote by C_j^3 , corresponding to stage 3 of the carpet. Figure 10 depicts such a supertile C_j^3 . Just as i corresponds to the position that C_i^2 is located in C_j^3 , the grout class j determines the position that C_j^3 will be located as a substage of a supertile corresponding to stage 4 of the carpet. Moreover, with glues strengths given Table 1, we note that grout tiles have been defined so that such $C_{(i,j)}^2$ supertiles bind before the “next iteration” of grout tiles can attach. In other words, $C_{(i,j)}^2$ supertiles bind for all i between 1 and 8 before a start-gadget can bind to the resulting supertile C_j^3 . For example, when $j = 1$, stage-binding glues are defined such that $h_{5,j}$ and $\hat{h}_{7,j}$ have strength 0. Therefore, any assembly sequence of C_1^3 ends with $C_{(8,1)}^2$ binding to a supertile consisting of $C_{(k,1)}^2$ for $1 \leq k \leq 7$. Hence, only after $C_{(8,1)}^2$ binds can a start-gadget bind to the resulting supertile. The cases where j is such that $2 \leq j \leq 8$ are similar.

Then, for i' such that $1 \leq i' \leq 8$, the glues that might allow (depending on i and i') some supertile $C_{(i,j)}^2$

to bind to another supertile $C_{(i',j)}^2$ are **stage-binding** glues separated by a distance of $2 = 3^{2-1} - 1$.² This distance is ensured by the locations of the **indicator** glues. As we will see, **stage-binding** glues will be reused as each consecutive stage of the carpet self-assembles. The distance between **stage-binding** glues will prevent supertiles corresponding to different fractal stages from binding.

Finally, the class of **grout** tiles that bind to some C_i^2 determines the presence and locations of **indicator** glues exposed by edges belonging to tiles of some C_j^3 . These **indicator** glues belonging to **grout** tiles are defined according to Table 2. The locations of **indicator** glues exposed by C_j^3 are analogous to the locations of these glues exposed by C_j^2 as shown in Figure 2, only the **indicator** glues of C_j^3 are at distance $8 = 3^{3-1} - 1$ apart. For example, referring to Figure 10, when $j = 1$, we note the presence of four **indicator** glues (two belonging to easternmost tiles and two belonging to southernmost tiles according to Table 2) exposed by C_1^3 that are distance 8 apart. Note the similarity between the locations of **indicator** glues in C_1^3 and in C_1^2 . **grout** tile types have been defined so that the same similarity is drawn between C_j^3 and C_j^2 for j between 1 and 8 (inclusive).

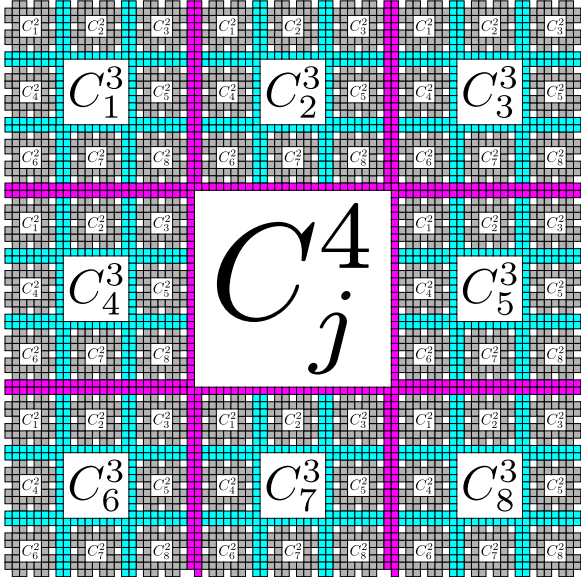


Fig. 11: A depiction of the portion of S^4 that is self-assembled by supertiles denoted by C_i^3 for i between 1 and 8 (inclusive) and some class j for j between 1 and 8 of **grout** tiles.

3.1.1.3 Self-assembly of stage s carpet for $s \geq 2$

Repurposing i , we now let C_j^3 be denoted by C_i^3 . Now, for each i and j with $1 \leq i, j \leq 8$, the 8 different classes of **grout** tile types can attach to each C_i^3 supertile to give supertiles $C_{(i,j)}^3$. The class **grout** class determines where the supertiles $C_{(i,j)}^3$ attach to self-assemble a supertile, C_j^4 , corresponding to a portion of S^4 . Such a C_j^4 is depicted in Figure 11. Moreover, the glues that allow some supertile $C_{(i,j)}^3$ to bind to another supertile $C_{(i',j)}^3$, for some i' say, are strength 1 or 0 glues, according to Table 1, separated by a distance of 8 apart. Note that the definitions of glues in Table 1 ensure that a C_j^4 supertile contains a supertile $C_{(i,j)}^3$ for each $1 \leq i \leq 8$ before a **start-gadget** supertile can attach to such a C_j^4 .

It is important to note that two **stage-binding** glues may be exposed on some strict subassembly of $C_{(i,j)}^3$, and therefore for some i and i' , two subassemblies of $C_{(i,j)}^3$ and $C_{(i',j)}^3$ may bind to form a subassembly of C_j^4 where some $C_{(i,j)}^3$ has only partially assembled. This can lead to cases of nondeterminism like the case depicted in Figure 12. We define glues belonging to **grout** tiles so that this does not prevent tiles from binding in locations corresponding to points of stage 2 at positions i and i' from completing assembly as a subassembly of C_j^4 . One such glue is shown in Figure 12 with label $g_{2,j}$. We also note that these glues do not permit tiles to bind in locations outside of locations in of tiles in positioned supertiles of C_j^4 . It is important to note that before such cases of nondeterminism can occur, all **stage-binding** glues of C_j^4 must be bound. Glues such as $g_{2,j}$ also ensure correct assembly of higher stage analogs of C_j^4 where analogous nondeterminism can also occur in the self-assembly of S^s for any higher stage $s > 3$.

Recursively repeating this process, we see that for any $i, j, s \in \mathbb{N}$ such that $1 \leq i, j \leq 8$ and $s > 2$, supertiles C_i^{s-1} corresponding to a portion of S^{s-1} (again, we are leaving room for **grout** tiles) self-assemble, and supertiles $C_{(i,j)}^{s-1}$ corresponding to C_i^{s-1} with the attachment of **grout** tiles all belonging to the j^{th} class of **grout** tile types self-assemble. Moreover, the supertiles $C_{(i,j)}^{s-1}$ with sufficient **grout** supertiles attached expose **stage-binding** glues that are at a distance of $3^{s-2} - 1$ apart (including glues with strength 0) that allow for the stable binding of these supertiles to form a supertile C_j^s corresponding to S^s . For $i' \in \mathbb{N}$ such that $1 \leq i' \leq 8$, since the distance between the 2 glues that allow for two supertiles $C_{(i,j)}^{s-1}$ and $C_{(i',j)}^{s-1}$ to bind is $3^{s-2} - 1$, one can observe that for $p, q \in \mathbb{N}$ such that $p, q \geq 2$, $C_{(i,j)}^p$ can bind to some $C_{(i',j')}^q$ for some i' and j' iff $p = q$ and $j = j'$. Moreover, by definition of the **grout** tile types, specific edges of tiles of C_j^s will expose **indica-**

² We are including glues with strength 0 here.

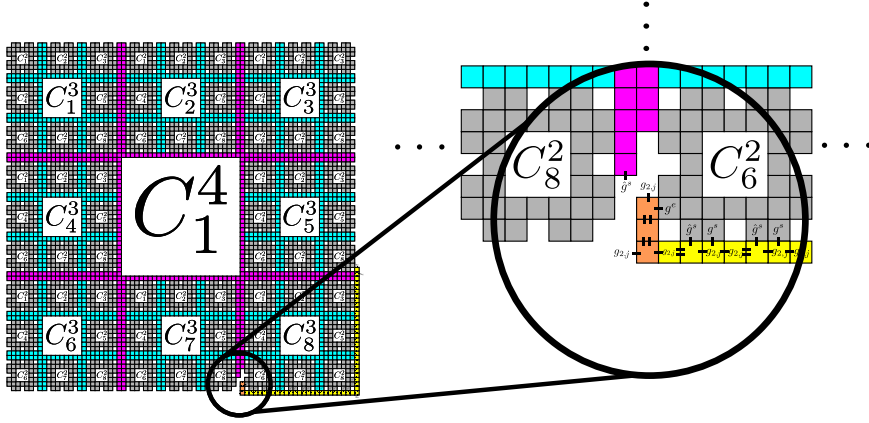


Fig. 12: An example where grout tiles have “turned a corner too early”. The grout tiles are shown in aqua, fuchsia, yellow, and orange. Note that C_8^3 and C_7^3 only have partial grout, though both have grout supertiles with stage-binding glues as is required for C_1^4 to be stable. In this case, when a grout supertile shown in orange binds, a $g_{2,j}$ is exposed that will eventually allow for grout tiles to continue to bind to the southernmost tiles of C_1^4 , but only after a sufficient number of grout supertiles bind to C_7^3 .

tor glues which are analogous to the indicating glues of C_j^{s-1} , only at distance $3^{s-1} - 1$ apart.

3.1.1.4 Correctness for the Sierpiński carpet construction

To prove that the tile set, T , gives a 2HAM TAS $\mathcal{T} = (T, 2)$ that finitely self-assembles \mathcal{S} , we note that by construction, for any finite producible supertile α of \mathcal{T} and for any $s \in \mathbb{N}$, there exists positive integers k , and j , and an assembly sequence $\alpha = \langle \alpha_i \rangle_{i=0}^k$ such that $\alpha_0 = \alpha$ and α_k is a C_j^s supertile. Therefore, any finite producible supertile α of \mathcal{T} has the shape of a subset of points in \mathcal{S} . Moreover, for any finite producible supertile α of \mathcal{T} , there exists an assembly sequence which starts with α and results in a supertile that has shape of \mathcal{S} . Therefore, we see that \mathcal{T} finitely self-assembles \mathcal{S} .

3.2 Self-assembly of 4-sided fractals

The construction that shows that any 4-sided fractal finitely self-assembles in the 2HAM at scale factor 1 (Theorem 1) is a generalization of the construction given in Section 3.1. Let G be the generator for a 4-sided fractal and recall the notation of L_G , R_G , B_G , and T_G defined in Section 2.2. We will describe a tile set T such that \mathbf{X} finitely self-assembles in the 2HAM system $\mathcal{T} = (T, 2)$. As an example, consider the generator in Figure 13a. Stage 2 of this fractal is depicted in Figure 13b.

Lemma 1 will be helpful for showing Theorem 1. This lemma states that if \mathbf{X} is a fractal with a generator G such that G only contains points along its

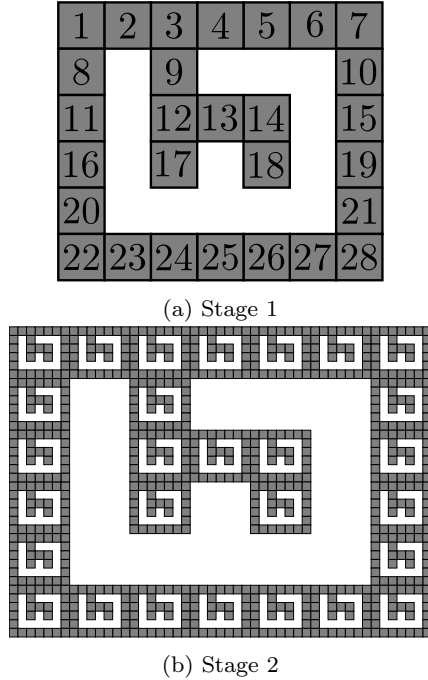


Fig. 13: Two stages of a 4-side fractal.

perimeter, then \mathbf{X} finitely self-assembles in the 2HAM at temperature 2.

Lemma 1 *Let \mathbf{X} be a 4-sided fractal with generator G such that $G \setminus (L_G \cup L_G \cup T_G \cup B_G) = \emptyset$. Then, there exists a 2HAM TAS $\mathcal{T}_{\mathbf{X}} = (T, 2)$ that finitely self-assembles \mathbf{X} .*

Proof (Sketch) For $s \in \mathbb{N}$, let X^s denote the s^{th} stage of \mathbf{X} , and let $r = |G|$. We note that the construction given in Section 3.1 generalizes in a straightforward way to give a tile set T satisfying Lemma 1. For example,

given the generator in Figure 14a, the modifications to the construction given in Section 3.1 are as follows. Once again, we consider two types of tiles in T which we call **initializer** tiles and **grout** tiles.

3.2.1 The *initializer* tile types for Lemma 1.

Let X'^2 denote the set of points in X^2 that are not on the perimeter of X^2 . Figure 14b depicts the points of an example X'^2 . **initializer** tiles of T now hard-code r different versions of X'^2 . For i between 1 and r (inclusive), we call these hard-coded supertiles Γ_i^2 . We note that as there is a Hamiltonian path in the full grid-graph of X'^2 , the glues of the **initializer** tiles can be specified so that Γ_i^2 completely assembles prior to being a subassembly of any other producible supertile.

In addition to hard-coding the shape of X'^2 , **initializer** tiles are specified so that once Γ_i^2 has completely self-assembled:

1. the north edges of northernmost tiles expose a g^n or \hat{g}^n such that the westernmost tile and every other tile from west to east exposes g^n and the remaining northernmost tiles expose a \hat{g}^n ,
2. the east edges of easternmost tiles expose a g^e or \hat{g}^e such that the northernmost tile and every other tile from north to south exposes g^e and the remaining easternmost tiles expose a \hat{g}^e ,
3. the south edges of southernmost tiles expose a g^s or \hat{g}^s such that the easternmost tile and every other tile from east to west exposes g^s and the remaining southernmost tiles expose a \hat{g}^s , and finally,
4. the west edges of westernmost tiles expose a g^w or \hat{g}^w such that the southernmost tile and every other tile from south to north exposes g^w and the remaining westernmost tiles expose a \hat{g}^w .

Edges of tiles in Γ_i^2 in “key locations” expose special glues \hat{g}_i and g_i which we call **indicator** glues. At these key locations, g_i is exposed instead of a g^n , g^s , g^e , or g^w and \hat{g}_i is exposed instead of a \hat{g}^n , \hat{g}^s , \hat{g}^e , or \hat{g}^w . These key locations of the tiles in Γ_i^2 that expose these glues are shown as red squares in Figure 14b. In general, these key locations will be the second to westernmost (resp. northernmost) and second to easternmost (resp. southernmost) tile locations of the northernmost (resp. easternmost) and southernmost (resp. westernmost) tile locations. Whether or not Γ_i^2 exposes **indicator** glues at these key locations depend on i . In particular, if the i^{th} location in G is adjacent to some other point that is north (resp. south, east, or west) of it, then, Γ_i^2 will expose **indicator** glues on the north (resp. south, east, or west) edges of tiles in northernmost (resp. southernmost, easternmost, or westernmost) key locations. **ind-**

icator glues in these key locations serve the same purpose to the **indicator** glues described in Section 3.1.1.

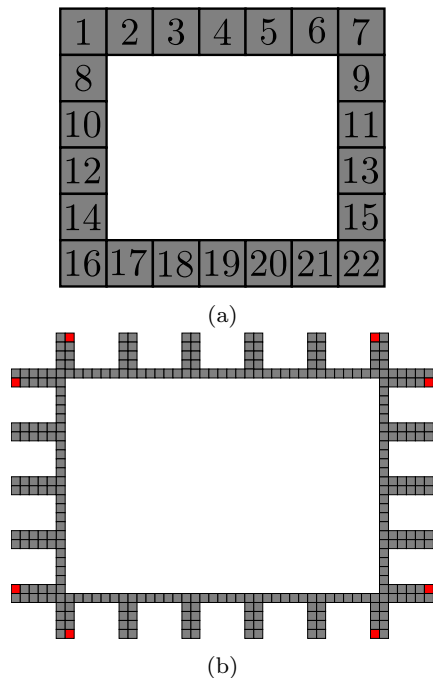


Fig. 14: (a) An example generator for the 4-sided fractals considered in Lemma 1. (b) A depiction of X'^2 . Red squares indicate possible locations of **indicator** glues \hat{g}_i and g_i .

3.2.2 The *grout* tile types for Lemma 1.

With the “base case” hard-coded to give Γ_i^2 , we are now ready to describe **grout** tiles. **grout** tiles will be almost identical to the **grout** tiles described in Section 3.1 with the exception that now the **grout** tiles must hard-code analogous though elongated versions of **grout** supertiles from Section 3.1. For example, elongated version of **start-gadget** supertiles that initiate the binding of **grout** tiles to Γ_1^2 is shown on the left in Figure 15. **grout** tiles of T are hard-coded to form similar “elongated” versions of **grout** supertiles to those described in Section 3.1. The only difference being that now these supertiles must span a distance of w_G between easternmost or westernmost tiles of Γ_i^2 and must span a distance of h_G between northernmost or southernmost tiles of Γ_i^2 in order to cooperatively bind.

Now, **grout** tiles fall into r different classes where each class corresponds to a position in G . For some class j between 1 and r (inclusive), **grout** tiles of class j bind to Γ_i^2 for each i such that $1 \leq i \leq r$. Then, **grout** tiles bind to the **indicator** glues of edges of tiles of Γ_i^2 in the key locations described above, the resulting

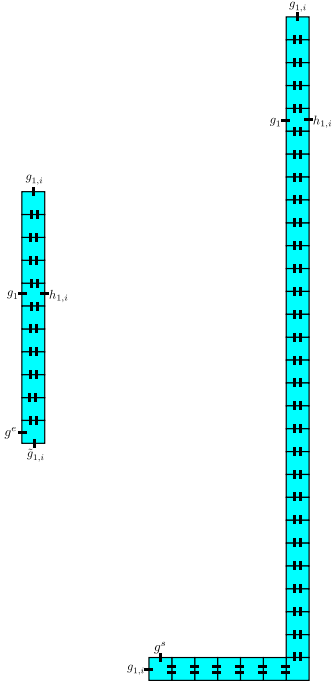


Fig. 15: “Elongated” versions of the supertiles that initiates the attachment of **grout** tiles to a supertile Γ_1^s (left), where $s \geq 3$, or Γ_1^2 (right). These are elongated versions of the **start-gadget** supertiles shown in Figure 3a.

supertiles, which we call $\Gamma_{(i,j)}^2$, further expose **stage-binding** glues on edges of tiles adjacent to tiles in key locations such that the presence of these glues enables the supertiles $\Gamma_{(i,j)}^2$ to bind and form a supertile that corresponds to the subsequent stage X^3 . Moreover, once all $\Gamma_{(i,j)}^2$ supertiles bind, a **start-gadget** supertile (like the one depicted on the left in Figure 15) can then initiate the binding of more **grout** tiles. Furthermore, by defining certain **stage-binding** glues to have strength 0, analogous to Table 1, we can enforce that such a supertile that initiates the binding of **grout** tiles (**start-gadget** supertiles) can bind only after all $\Gamma_{(i,j)}^2$ supertiles are subassemblies of the same supertile. We call this latter supertile, that corresponds to X^3 , Γ_j^3 . For a stage $s > 3$, the self-assembly of supertiles, Γ_j^s , which correspond to X^s is similar to the self-assembly of supertiles C_j^s for the Sierpiński carpet given in Section 3.1.1. Finally, glue definition similar to Table 2 can be given for **grout** tiles so that appropriate **indicator** glues are exposed by tiles belonging to Γ_j^3 to ensure that Γ_j^3 exposes **indicator** glues so that the next iteration of **grout** supertiles to bind expose **stage-binding** glues in specific locations. These specific locations are chosen so that for $s \geq 2$, the distance between the **indicator** glues of some Γ_j^s is a strictly increasing function of s , which ensures that two such supertiles can bind iff they correspond to the same stage of the fractal \mathbf{X} .

Similar to the Sierpiński carpet construction, we can see that the **initializer** tiles self-assemble supertiles that correspond to X^2 and that **grout** tiles can attach to supertiles that correspond to X^s for some stage $s \geq 2$ to form supertiles that bind to yield a supertile corresponding to X^{s+1} . Therefore, with tiles T , the 2HAM system $\mathcal{T} = (T, 2)$ finitely self-assembles \mathbf{X} . Therefore, Lemma 1 holds. Now we are ready to prove Theorem 1.

3.3 Proof of Theorem 1 (Sketch)

Let \mathbf{X} be a 4-sided dssf with generator G and let $r = |G|$. In this section, we give a sketch of the proof of Theorem 1 by describing how to modify the tile set given in the proof of Lemma 1 to obtain a tile set T such that the 2HAM TAS $\mathcal{T} = (T, 2)$ finitely self-assembles \mathbf{X} . Figure 13a gives an example of a generator G where we enumerate the points of G from left to right, from top to bottom. Now let $G_{int} = G \setminus (L_G \cup R_G \cup T_G \cup B_G)$ (i.e. the points of G that are not on the perimeter of G), and let G_{bdry} be $G \setminus G_{int}$.

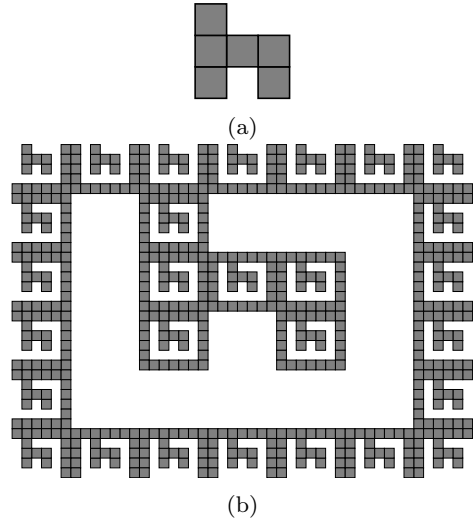


Fig. 16: (a) A depiction of \mathcal{G}_1^- for the generator in Figure 13a. (b) A depiction of \mathcal{G}^- for the generator in Figure 13a.

By Lemma 1 there is a 2HAM system \mathcal{T}' which finitely self-assembles the dssf with generator G_{bdry} . Let T' be the tile set for \mathcal{T}' as described in the construction for Lemma 1. We will show how to modify the tile set T' to obtain T .

3.3.1 Self-assembly of stage 2 for 4-sided fractals

Let \mathcal{G}_1 denote the full grid-graph of G and let \mathcal{G}_1^- denote the full grid-graph of G_{int} . Note that it is not necessary for \mathcal{G}_1^- to be connected. Also note that \mathcal{G}_1^- may be

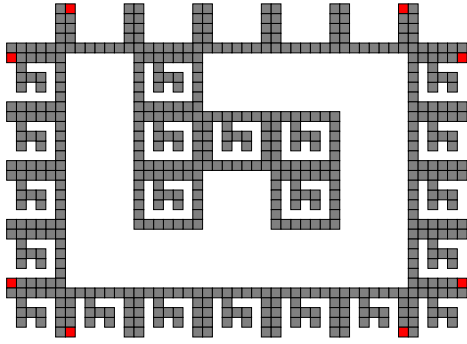


Fig. 17: A depiction of Γ_i^2 . This is the portion of the second stage of the fractal with generator in Figure 13a that is hard-coded to self-assemble. It is analogous to the second stages that assemble shown in Figure 14b for the construction for Lemma 1.

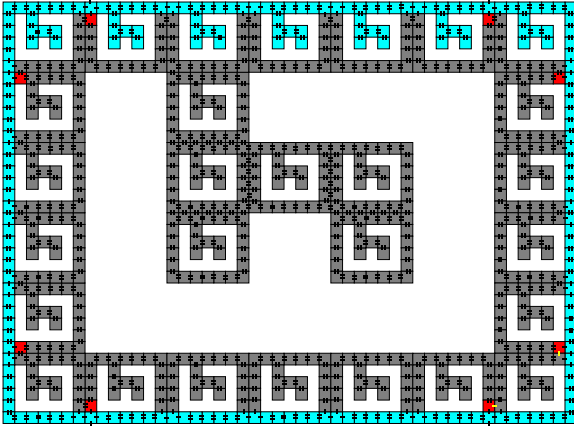


Fig. 18: A depiction of $\Gamma_{(12,j)}^2$ for some $j \in \mathbb{N}$ corresponding to the j class of **grout**. Note the glues that are exposed on tiles adjacent to tiles with indicator glues (red tiles). In this case, as position 12 in the generator G is in G_{int} , **grout** supertiles bind to on all four sides of Γ_{12}^2 . **grout** supertiles that bind to indicator glues expose **stage-binding** glues which allow $\Gamma_{(12,j)}^2$ to bind in position 12 during the self-assembly of a Γ_j^3 supertile.

empty if $G = L_G \cup R_G \cup T_G \cup B_G$ as in the case for the Sierpiński carpet dssf. An example of \mathcal{G}_1^- for the generator shown in Figure 13a is shown in Figure 16a where vertices correspond to squares and there is assumed to be an edge between two vertices iff these squares abut. Now let \mathcal{G} denote the full grid-graph of X^2 . Let \mathcal{G}^- be the (not necessarily connected) graph obtained by removing the northernmost, southernmost, easternmost, and westernmost points from \mathcal{G} . For the generator given in Figure 13a, \mathcal{G}^- is shown in Figure 16b. Finally, let \mathcal{G}_c be the connected component of \mathcal{G}^- that is not equal to a connected component of \mathcal{G}_1^- up to translation. See Figure 17 for an example of \mathcal{G}_c for the generator shown in Figure 13a.

Then, the **initializer** tiles of T are hard-coded to self-assemble r different versions of \mathcal{G}_c which we call Γ_i^2 for $1 \leq i \leq r$. Similar to the **initializer** tiles described in the proof of Lemma 1, each Γ_i^2 contains tiles in key locations (defined as in Lemma 1) that expose **indicator** glues that depend on the value of i . These **initializer** tiles can be thought of as being equivalent to the **initializer** tiles of T' , appropriately modified with additional glues and additional tiles that hard-code the stage 1 subassemblies of **initializer** supertiles whose positions in the Γ_i^2 correspond to the points of G_{int} . In the example in Figure 17, these additional tiles self-assemble at locations 9, 12, 13, 14, 17, and 18 within stage-1 subassemblies at locations 8 through 28, as well as self-assemble entire stage-1 subassemblies at locations 9, 12, 13, 14, 17, and 18. Figure 17 depicts the locations of tiles of Γ_i^2 for the generator in Figure 13a, where red tiles may contain edges with **indicator** glues.

3.3.2 Tile types for **grout** tiles.

The **grout** tile types of T consist of tile types that are equivalent to the **grout** tile types of T' with additional glues along with additional tile types that hard-code the appropriate stage 1 growth that complete any subassemblies that represent X^1 . Figure 18 gives an example of Γ_{12}^2 with complete **grout**. In this particular example, **grout** tiles have been hard-coded to place tiles in locations corresponding to X^1 as the **grout** tiles bind to the northernmost tiles of Γ_{12}^2 . **grout** tiles are added for each i between 1 and r (inclusive) and as in Figure 18, **grout** tiles may bind to some Γ_i^2 where i corresponds to a point in G_{int} . In this case, **grout** tiles can be defined to completely surround Γ_i^2 (or Γ_i^s for $s > 2$) and expose appropriate **stage-binding** glues at key locations. **stage-binding** glues ensure that for all i and j both between 1 and 8 (inclusive), once a sufficient number of **grout** tiles bind to each Γ_i^2 , the resulting supertiles, which we again call $\Gamma_{(i,j)}^2$ (or $\Gamma_{(i,j)}^s$ for $s > 2$) can bind to yield a supertile corresponding to X^3 (or X^s for $s > 2$). We call this latter supertile Γ_j^3 (or Γ_j^{s+1} for $s > 2$). Figure 19 depicts Γ_j^3 .

As \mathcal{T} is based on \mathcal{T}' , the assembly sequences of each system share similarities that are important to note. For a stage $s \in \mathbb{N}$, and j such that $1 \leq j \leq 8$, let $\Gamma_j^{s'}$ be the supertile producible in \mathcal{T}' corresponding to $X^{s'}$. Note that as the tile types in T are based on tile types in T' , in an assembly sequence for Γ_j^s , the tiles in Γ_j^s with locations (up to some fixed positioning of the supertile) corresponding to points of G_{bdry} (at any stage) must bind in an order corresponding to some assembly sequence of $\Gamma_j^{s'}$. In other words, the portion of the fractal

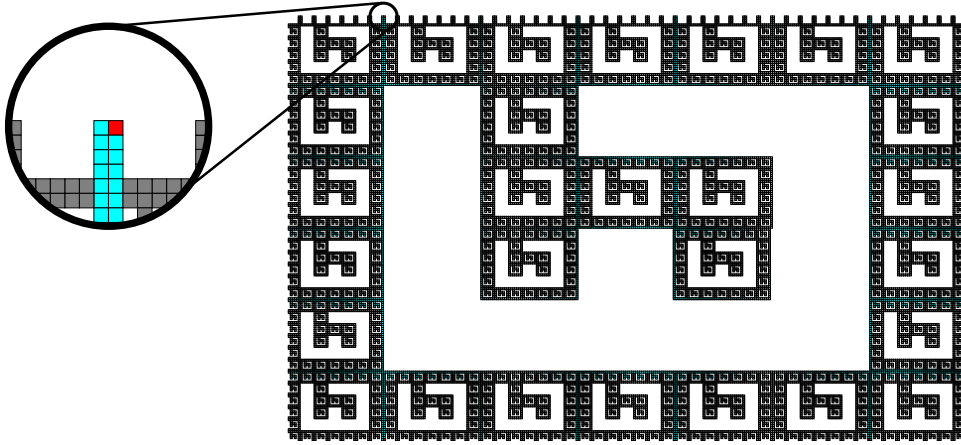


Fig. 19: A schematic picture of Γ_j^3 . Note the red tile locations where tiles with indicator glues (red tiles) will be present. Also note that **grout** supertiles that bind to the northernmost tiles of the supertile depicted here hard-code the placement of tiles in locations corresponding to X^1 .

\mathbf{X} equal to \mathbf{X}' must self-assemble following an assembly sequence in \mathcal{T} analogous to an assembly sequence in \mathcal{T}' . The analogous assembly sequence can be obtained by ignoring any supertile combinations that involve a supertile corresponding to points of G_{int} at any stage. Therefore, \mathbf{X}' finitely self-assembles in \mathcal{T} . The additional **initializer** and **grout** tiles are defined to “fill in” tile locations in \mathbf{X} that are not in \mathbf{X}' by non-deterministically binding, following one of many possible assembly sequences.

Finally, the **initializer** tiles assemble a supertile that corresponds to X^2 , and **grout** supertiles tiles can attach to supertiles that correspond to X^s for some stage $s \geq 2$ to form supertiles that bind to yield a supertile corresponding to X^{s+1} . Therefore, with tiles T , the 2HAM system $\mathcal{T} = (T, 2)$ finitely self-assembles \mathbf{X} . Therefore, Theorem 1 holds.

4 A 3-sided Fractal That Does Not Finitely Self-assemble

In this section we prove that there exist 3-sided fractals that do not finitely self-assemble in the 2HAM.

Theorem 2 *There exists a 3-sided fractal \mathbf{X} for which there is no 2HAM TAS $\mathcal{T}_{\mathbf{X}} = (T, \tau)$ that finitely self-assembles \mathbf{X} for any temperature $\tau \in \mathbb{N}$.*

To prove Theorem 2, we consider the fractal with generator $G = \{(0, 4), (1, 4), (2, 4), (3, 4), (0, 3), (2, 3), (0, 2), (2, 2), (0, 1), (0, 0), (1, 0), (2, 0), (3, 0)\}$. Stages 1 and 2 of this fractal are shown in Figure 20. We refer to this fractal as \mathbf{X} . For a stage $s \in \mathbb{N}$, we refer to the i^{th} position of X^s as X_i^s where $1 \leq i \leq 13$ (Figure 20a). We call a supertile with shape X^s γ^s , and when such a

supertile is a subassembly of some γ^{s+1} and corresponds to points location i , we denote such assemblies by γ_i^s .

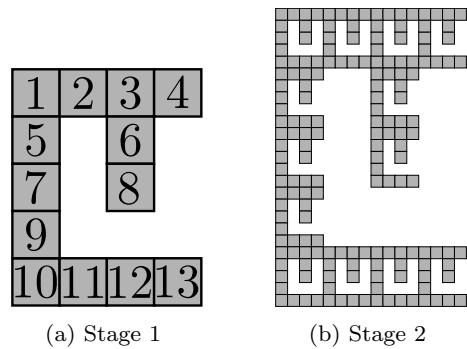


Fig. 20: X^1 and X^2

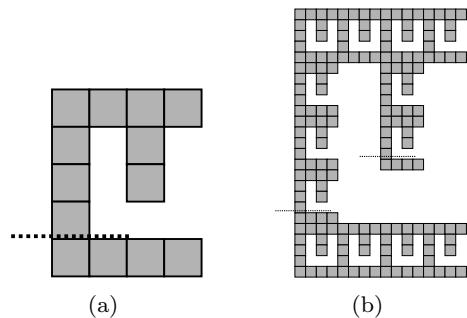


Fig. 21: Strength τ cuts in γ^1 and γ^2

For the sake of contradiction, assume that $\mathcal{T}_{\mathbf{X}} = (T, \tau)$ is a 2HAM TAS such that \mathbf{X} finitely self-assembles in $\mathcal{T}_{\mathbf{X}}$. Consider any 2HAM TAS $\mathcal{T}_{\mathbf{X}} = (T, \tau)$. We show that $\mathcal{T}_{\mathbf{X}}$ does not finitely self-assemble \mathbf{X} by showing

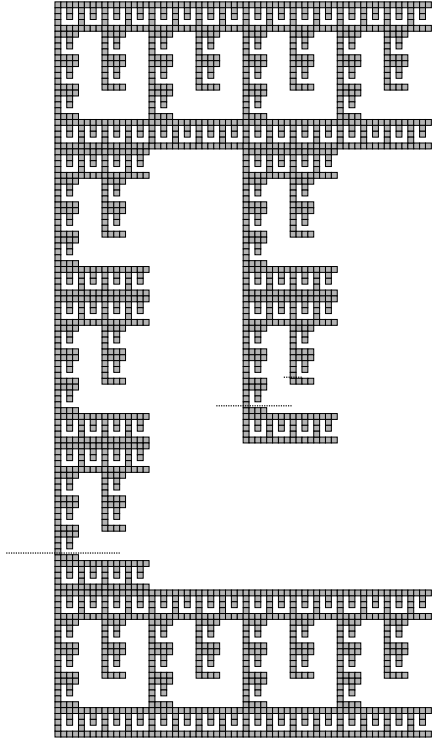


Fig. 22: There are at least s strength τ cuts within each supertile γ^s . Here γ^3 with 3 strength τ cuts is shown. The subassembly to the south of the rightmost cut is referred to as β_1 , the subassembly to the south of the next rightmost cut as β_2 , and the subassembly to the south of the leftmost cut as β_3 .

that there is a producible supertile $\alpha \in \mathcal{A}_{\square}[\mathcal{T}_{\mathbf{X}}]$ that does not have the shape of any subset of \mathbf{X} .

Then, for any $s \in \mathbb{N}$, and for every supertile α such that α contains a γ^s subassembly, there is a stage 1 subassembly γ^1 of γ_9^s such that this stage 1 subassembly contains a strength τ cut between γ_9^1 and γ_{10}^1 that separates some $\gamma_{10}^s, \gamma_{11}^s, \gamma_{12}^s$, and γ_{13}^s subassemblies, along with a sequence of subassemblies $\gamma_{10}^i, \gamma_{11}^i, \gamma_{12}^i$, and γ_{13}^i , $i < s$, from the rest of γ^s . For an example of such a cut, see the bottom left cuts shown in Figure 21b for $s = 2$ and in Figure 22 for $s = 3$. Then note that for any $s > 2$, γ_8^s has a γ^{s-1} subassembly which contains a similar strength τ cut between two tiles γ_9^1 and γ_{10}^1 in the γ^1 subassembly directly above γ_{10}^{s-1} .

Then γ_8^s has a subassembly γ^1 which contains a single strength τ cut between γ_9^1 and γ_{10}^1 (shown as the cut on the right in Figure 21b). We also note that when $s = 1$ there is one strength τ cut between γ_9^s and γ_{10}^s . Therefore every supertile α such that there exists $A \in \alpha$ with $X^s \subseteq A$ contains a sequence of s strength τ cuts between positions 9 and 10 of s distinct stage 1 subassemblies. An example of this for $s = 3$ is shown in Figure 22.

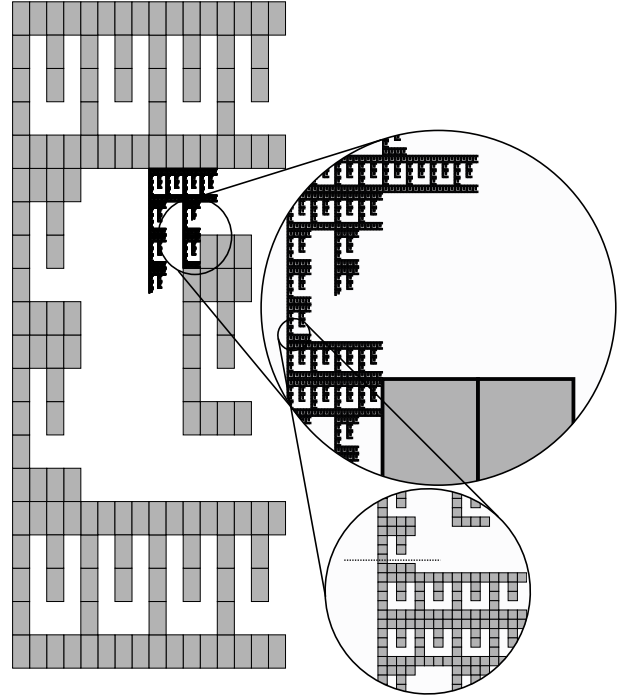


Fig. 23: An example of erroneous binding within γ^5 . Because of the large number of tiles some of the γ^3 subassemblies are shown as rectangles. In this example, a τ strength cut is shown in the bottom right circle. The subassembly of γ^5 containing the tile to the north of this cut is α_2 and the subassembly containing the tile to the south of this cut is $\beta_{s'}$.

Let g be the number of tiles in T . Consider a producible supertile α such that there exists $A \in \alpha$ with $X^{g+2} \subseteq A$. Within α there is a γ^{g+2} subassembly with some γ_6^{g+1} as a subassembly. As we have shown, this γ_6^{g+1} contains a sequence of $g + 1$ strength τ cuts, each consisting of a single glue. By the pigeonhole principle, there are at least two such cuts that consist of the same single τ strength glue. Let the subassembly to the south of the cut within γ^1 be called β_1 , the subassembly to the south of the cut within γ_9^2 be called β_2 , etc., with the subassembly to the south of the cut within γ_9^{g+1} called β_{g+1} (see Figure 22 for an example of β_1, β_2 , and β_3). Consider two cuts directly above β_s and $\beta_{s'}$ with $s' > s$ that contain the same glue. Let α_2 be α with subassemblies of $\beta_s, \beta_{s+1}, \dots, \beta_{s'}$ removed. We will show that α_2 and $\beta_{s'}$ are producible assemblies. Additionally, we notice that between X_8^{g+2} and X_{12}^{g+2} there is enough room to fit an entire stage X^{g+1} , and since $s' \leq g + 1$, erroneous binding of α_2 and $\beta_{s'}$ cannot be prevented. Figure 23 depicts an example of such erroneous binding within a γ^5 supertile. Hence α_2 and $\beta_{s'}$ are τ -combinable into some supertile $\chi \in \mathcal{A}[\mathcal{T}_{\mathbf{X}}]$. Then, note that for all $A \in \chi$, the set of all tile locations of tiles in A is not contained in $\subseteq \mathbf{X}$. Therefore, $\mathcal{T}_{\mathbf{X}}$ does not finitely self-assemble \mathbf{X} .

To complete the proof, we now show that the sub-assemblies α_2 and $\beta_{s'}$ are producible. If one of α_2 or $\beta_{s'}$ is not producible, then the binding graph of that one must contain a cut with strength less than τ . However, since every β_i , $1 \leq i \leq g + 1$, is connected to α by a single strength- τ glue between two single tiles, if the the binding graph of α_2 or $\beta_{s'}$ contains a cut with strength less than τ , then α would contain the same cut with strength less than τ . This contradicts the assumption that α is producible. Hence $\alpha_2, \beta_{s'} \in \mathcal{A}[\mathcal{T}_X]$. Thus, Theorem 2 holds.

5 Conclusion

Theorem 1 shows that any 4-sided dssf finitely self-assembles in the 2HAM at temperature 2 and with scale factor 1. Theorem 2 shows that there exists a 3-sided fractal that does not finitely self-assemble in any 2HAM system at any temperature. For a 4-sided fractal generator G , the presence of a Hamiltonian cycle in the full grid graph of the points on the perimeter of G proved helpful in our construction. Similar techniques to those described in Section 3 might be used to show that a much more general class of fractals finitely self-assembles in the 2HAM at temperature 2 with scale factor 1. In particular, a fractal belonging to this class can be described as having a generator such that 1) the full grid-graph of the generator contains a Hamiltonian cycle through each point in the generator and 2) the northernmost, southernmost, easternmost, and westernmost points of the generator each contain 2 distinct points. An example of such a fractal is shown in Figure 24

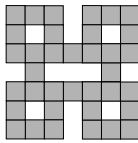


Fig. 24: Do fractals with generators like the one depicted in this figure finitely self-assemble in the 2HAM?

6 Acknowledgements

The authors would like to thank the anonymous reviewers for their time and effort in helping to improve this paper.

References

1. Z. Abel, N. Benbernou, M. Damian, E. Demaine, M. Demaine, R. Flatland, S. Kominers, and R. Schweller. Shape

replication through self-assembly and RNase enzymes. In *SODA 2010: Proceedings of the Twenty-first Annual ACM-SIAM Symposium on Discrete Algorithms*, Austin, Texas, 2010. Society for Industrial and Applied Mathematics.

2. K. Barth, D. Furcy, S. M. Summers, and P. Totzke. Scaled tree fractals do not strictly self-assemble. In *Unconventional Computation & Natural Computation (UCNC) 2014, University of Western Ontario, London, Ontario, Canada July 14-18, 2014*, pages 27–39, 2014.
3. S. Cannon, E. D. Demaine, M. L. Demaine, S. Eisenstat, M. J. Patitz, R. T. Schweller, S. M. Summers, and A. Winslow. Two hands are better than one (up to constant factors): Self-assembly in the 2ham vs. atam. In N. Portier and T. Wilke, editors, *STACS*, volume 20 of *LIPICs*, pages 172–184. Schloss Dagstuhl - Leibniz-Zentrum fuer Informatik, 2013.
4. C. Chalk, E. D. Demaine, M. L. Demaine, E. Martinez, R. Schweller, L. Vega, and T. Wylie. Universal shape replicators via self-assembly with attractive and repulsive forces. In *Proceedings of the Twenty-Eighth Annual ACM-SIAM Symposium on Discrete Algorithms*, SODA '17, pages 225–238, Philadelphia, PA, USA, 2017. Society for Industrial and Applied Mathematics.
5. C. T. Chalk, D. A. Fernandez, A. Huerta, M. A. Maldonado, R. T. Schweller, and L. Sweet. Strict self-assembly of fractals using multiple hands. *Algorithmica*, pages 1–30, 2015.
6. Q. Cheng, G. Aggarwal, M. H. Goldwasser, M.-Y. Kao, R. T. Schweller, and P. M. de Espanés. Complexities for generalized models of self-assembly. *SIAM Journal on Computing*, 34:1493–1515, 2005.
7. M. Cook, Y. Fu, and R. T. Schweller. Temperature 1 self-assembly: Deterministic assembly in 3D and probabilistic assembly in 2D. In *SODA 2011: Proceedings of the 22nd Annual ACM-SIAM Symposium on Discrete Algorithms*. SIAM, 2011.
8. E. D. Demaine, M. L. Demaine, S. P. Fekete, M. Ishaque, E. Rafalin, R. T. Schweller, and D. L. Souvaine. Staged self-assembly: nanomanufacture of arbitrary shapes with $O(1)$ glues. *Natural Computing*, 7(3):347–370, 2008.
9. E. D. Demaine, M. L. Demaine, S. P. Fekete, M. J. Patitz, R. T. Schweller, A. Winslow, and D. Woods. One tile to rule them all: Simulating any tile assembly system with a single universal tile. In *Proceedings of the 41st International Colloquium on Automata, Languages, and Programming (ICALP 2014)*, IT University of Copenhagen, Denmark, July 8-11, 2014, volume 8572 of *LNCS*, pages 368–379, 2014.
10. E. D. Demaine, M. J. Patitz, T. A. Rogers, R. T. Schweller, S. M. Summers, and D. Woods. The two-handed tile assembly model is not intrinsically universal. *Algorithmica*, 74(2):812–850, Feb 2016.
11. E. D. Demaine, M. J. Patitz, R. T. Schweller, and S. M. Summers. Self-Assembly of Arbitrary Shapes Using RNase Enzymes: Meeting the Kolmogorov Bound with Small Scale Factor (extended abstract). In T. Schwentick and C. Dürr, editors, *28th International Symposium on Theoretical Aspects of Computer Science (STACS 2011)*, volume 9 of *Leibniz International Proceedings in Informatics (LIPIcs)*, pages 201–212, Dagstuhl, Germany, 2011. Schloss Dagstuhl–Leibniz-Zentrum fuer Informatik.
12. D. Doty, L. Kari, and B. Masson. Negative interactions in irreversible self-assembly. In *DNA 16: Proceedings of The Sixteenth International Meeting on DNA Computing and Molecular Programming*, Lecture Notes in Computer Science, pages 37–48. Springer, 2010.

13. D. Doty, J. H. Lutz, M. J. Patitz, R. T. Schweller, S. M. Summers, and D. Woods. The tile assembly model is intrinsically universal. In *Proceedings of the 53rd Annual IEEE Symposium on Foundations of Computer Science*, FOCS 2012, pages 302–310, 2012.
14. D. Doty, M. J. Patitz, D. Reishus, R. T. Schweller, and S. M. Summers. Strong fault-tolerance for self-assembly with fuzzy temperature. In *Proceedings of the 51st Annual IEEE Symposium on Foundations of Computer Science (FOCS 2010)*, pages 417–426, 2010.
15. D. Doty, M. J. Patitz, and S. M. Summers. Limitations of self-assembly at temperature 1. In *Proceedings of The Fifteenth International Meeting on DNA Computing and Molecular Programming (Fayetteville, Arkansas, USA, June 8-11, 2009)*, pages 283–294, 2009.
16. S. P. Fekete, J. Hendricks, M. J. Patitz, T. A. Rogers, and R. T. Schweller. Universal computation with arbitrary polyomino tiles in non-cooperative self-assembly. In *Proceedings of the Twenty-Sixth Annual ACM-SIAM Symposium on Discrete Algorithms (SODA 2015), San Diego, CA, USA January 4-6, 2015*, pages 148–167, 2015.
17. K. Fujibayashi, R. Hariadi, S. H. Park, E. Winfree, and S. Murata. Toward reliable algorithmic self-assembly of DNA tiles: A fixed-width cellular automaton pattern. *Nano Letters*, 8(7):1791–1797, 2007.
18. O. Gilber, J. Hendricks, M. J. Patitz, and T. A. Rogers. Computing in continuous space with self-assembling polygonal tiles. In *Proceedings of the Twenty-Seventh Annual ACM-SIAM Symposium on Discrete Algorithms (SODA 2016), Arlington, VA, USA January 10-12, 2016*, pages 937–956, 2016.
19. J. Hendricks, J. Obseht, M. J. Patitz, and S. M. Summers. Hierarchical growth is necessary and (sometimes) sufficient to self-assemble discrete self-similar fractals. In preparation.
20. J. Hendricks, M. Olsen, M. J. Patitz, T. A. Rogers, and H. Thomas. Hierarchical self-assembly of fractals with signal-passing tiles (extended abstract). In *Proceedings of the 22nd International Conference on DNA Computing and Molecular Programming (DNA 22), Ludwig-Maximilians-Universitt, Munich, Germany September 4-8, 2016*, pages 82–97.
21. J. Hendricks, M. J. Patitz, and T. Rogers. Reflections on tiles (in self-assembly). In *Proceedings of The 21st International Conference on DNA Computing and Molecular Programming (Harvard University, Aug 17-21, 2015)*, 2015. to appear.
22. J. Hendricks, M. J. Patitz, and T. A. Rogers. Universal simulation of directed systems in the abstract tile assembly model requires undirectedness. In *Proceedings of the 57th Annual IEEE Symposium on Foundations of Computer Science (FOCS 2016), New Brunswick, New Jersey, USA October 9-11, 2016*, pages 800–809.
23. J. Hendricks, M. J. Patitz, and T. A. Rogers. The simulation powers and limitations of higher temperature hierarchical self-assembly systems. *Fundam. Inform.*, 155(1-2):131–162, 2017.
24. N. Jonoska and D. Karpenko. Active tile self-assembly, self-similar structures and recursion. Technical Report 1211.3085, Computing Research Repository, 2012.
25. N. Jonoska and D. Karpenko. Active tile self-assembly, part 1: Universality at temperature 1. *International Journal of Foundations of Computer Science*, 25(02):141–163, 2014.
26. N. Jonoska and D. Karpenko. Active tile self-assembly, part 2: Self-similar structures and structural recursion. *International Journal of Foundations of Computer Science*, 25(02):165–194, 2014.
27. M.-Y. Kao and R. T. Schweller. Reducing tile complexity for self-assembly through temperature programming. In *Proceedings of the 17th Annual ACM-SIAM Symposium on Discrete Algorithms (SODA 2006), Miami, Florida, Jan. 2006, pp. 571-580*, 2007.
28. S. Kautz and B. Shuttters. Self-assembling rulers for approximating generalized sierpinski carpets. *Algorithmica*, 67(2):207–233, 2013.
29. S. M. Kautz and J. I. Lathrop. Self-assembly of the Sierpinski carpet and related fractals. In *Proceedings of The Fifteenth International Meeting on DNA Computing and Molecular Programming (Fayetteville, Arkansas, USA, June 8-11, 2009)*, pages 78–87, 2009.
30. J. I. Lathrop, J. H. Lutz, and S. M. Summers. Strict self-assembly of discrete Sierpinski triangles. *Theoretical Computer Science*, 410:384–405, 2009.
31. A. Luchsinger, R. Schweller, and T. Wylie. Self-assembly of shapes at constant scale using repulsive forces. *Natural Computing*, Aug 2018.
32. J. H. Lutz and B. Shuttters. Approximate self-assembly of the sierpinski triangle. *Theory Comput. Syst.*, 51(3):372–400, 2012.
33. P. Meunier and D. Woods. The non-cooperative tile assembly model is not intrinsically universal or capable of bounded turing machine simulation. In *Proceedings of the 49th Annual ACM SIGACT Symposium on Theory of Computing, STOC 2017, Montreal, QC, Canada, June 19-23, 2017*, pages 328–341, 2017.
34. P.-E. Meunier, M. J. Patitz, S. M. Summers, G. Theyssier, A. Winslow, and D. Woods. Intrinsic universality in tile self-assembly requires cooperation. In *Proceedings of the ACM-SIAM Symposium on Discrete Algorithms (SODA 2014), (Portland, OR, USA, January 5-7, 2014)*, pages 752–771, 2014.
35. J. E. Padilla, M. J. Patitz, R. T. Schweller, N. C. Seeman, S. M. Summers, and X. Zhong. Asynchronous signal passing for tile self-assembly: Fuel efficient computation and efficient assembly of shapes. *International Journal of Foundations of Computer Science*, 25(4):459–488, 2014.
36. M. J. Patitz. An introduction to tile-based self-assembly and a survey of recent results. *Natural Computing*, 13(2):195–224, 2014.
37. M. J. Patitz, R. T. Schweller, and S. M. Summers. Exact shapes and turing universality at temperature 1 with a single negative glue. In *Proceedings of the 17th international conference on DNA computing and molecular programming, DNA’11*, pages 175–189, 2011.
38. M. J. Patitz and S. M. Summers. Self-assembly of discrete self-similar fractals. *Natural Computing*, 1:135–172, 2010.
39. P. W. Rothmund, N. Papadakis, and E. Winfree. Algorithmic self-assembly of DNA Sierpinski triangles. *PLoS Biology*, 2(12):2041–2053, 2004.
40. P. W. K. Rothmund, N. Papadakis, and E. Winfree. Algorithmic self-assembly of dna sierpinski triangles. *PLoS Biol*, 2(12):e424, 12 2004.
41. P. W. K. Rothmund and E. Winfree. The program-size complexity of self-assembled squares (extended abstract). In *STOC ’00: Proceedings of the thirty-second annual ACM Symposium on Theory of Computing*, pages 459–468, Portland, Oregon, United States, 2000. ACM.
42. S. M. Summers. Reducing tile complexity for the self-assembly of scaled shapes through temperature programming. *Algorithmica*, 63(1-2):117–136, June 2012.
43. E. Winfree. *Algorithmic Self-Assembly of DNA*. PhD thesis, California Institute of Technology, June 1998.

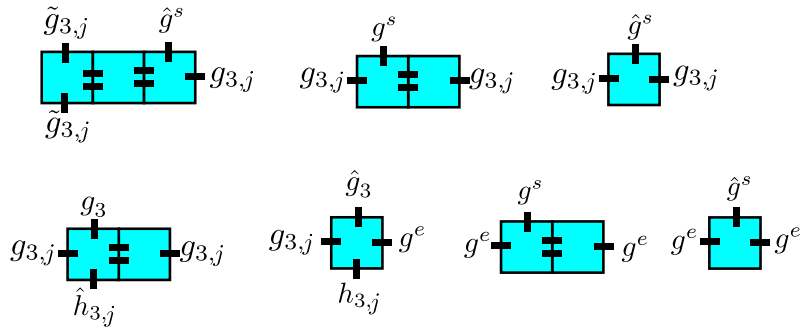


Fig. 27: The tiles and supertiles that bind to the south side of C_3^s for $s \geq 2$.

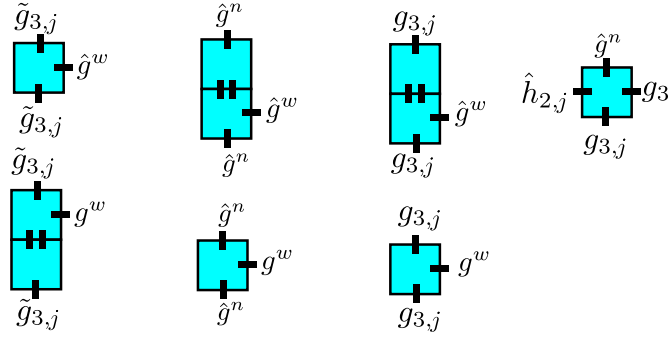


Fig. 28: The tiles and supertiles that bind to the west side of C_3^s for $s \geq 2$.

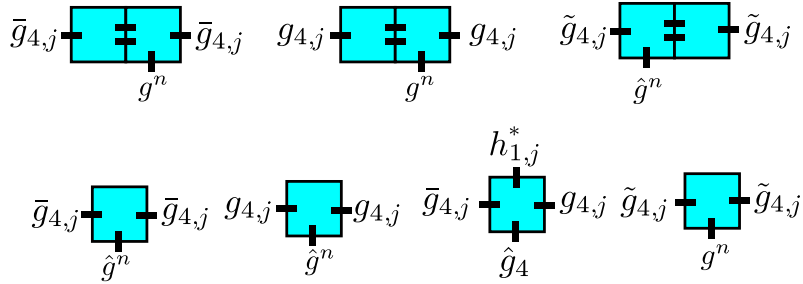


Fig. 29: The tiles and supertiles that bind to the north side of C_4^s for $s \geq 2$.

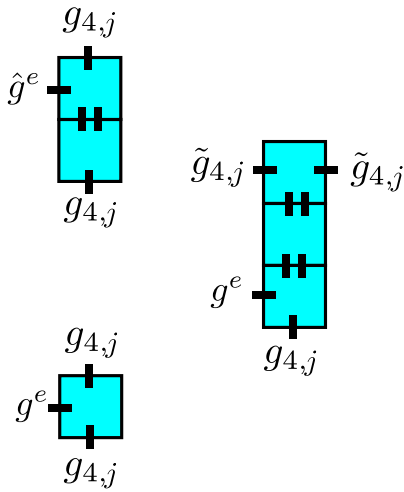


Fig. 30: The tiles and supertiles that bind to the east side of C_4^s for $s \geq 2$.

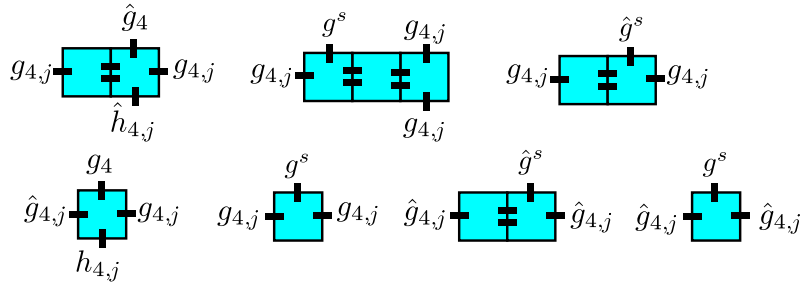


Fig. 31: The tiles and supertiles that bind to the south side of C_4^s for $s \geq 2$.

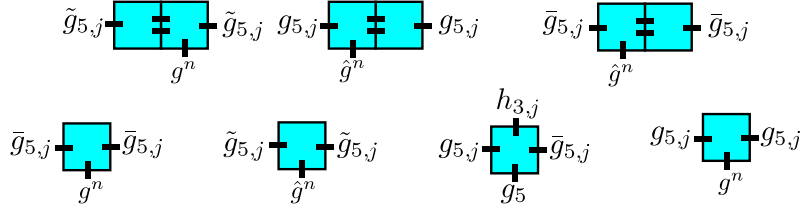


Fig. 32: The tiles and supertiles that bind to the north side of C_5^s for $s \geq 2$.

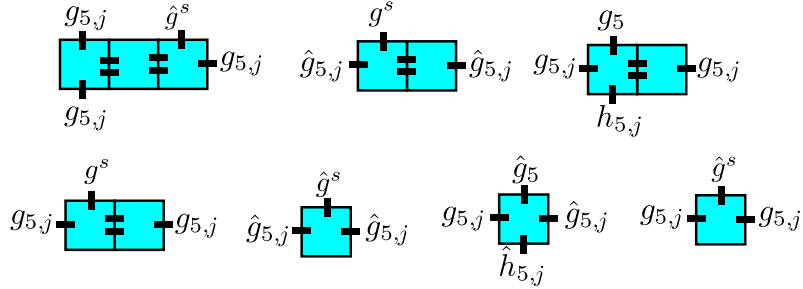


Fig. 33: The tiles and supertiles that bind to the south side of C_5^s for $s \geq 2$.

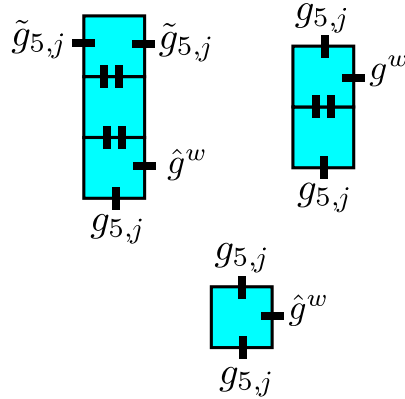


Fig. 34: The tiles and supertiles that bind to the west side of C_5^s for $s \geq 2$.

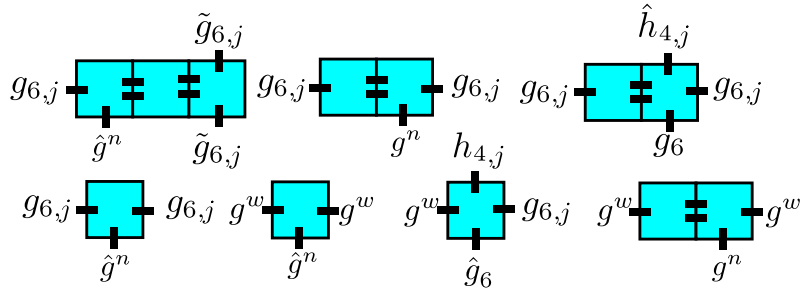


Fig. 35: The tiles and supertiles that bind to the north side of C_6^s for $s \geq 2$.

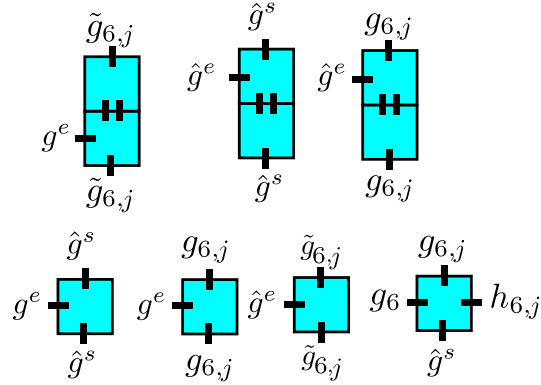


Fig. 36: The tiles and supertiles that bind to the east side of C_6^s for $s \geq 2$.

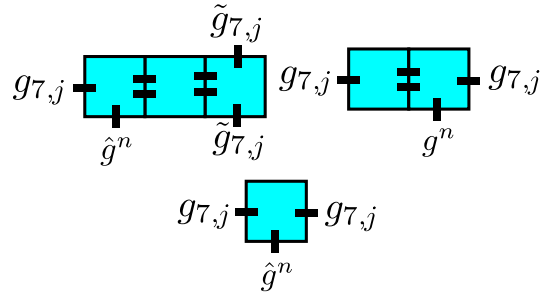


Fig. 37: The tiles and supertiles that bind to the north side of C_7^s for $s \geq 2$.

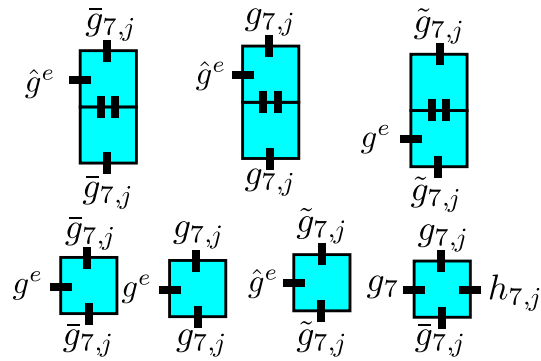


Fig. 38: The tiles and supertiles that bind to the east side of C_7^s for $s \geq 2$.

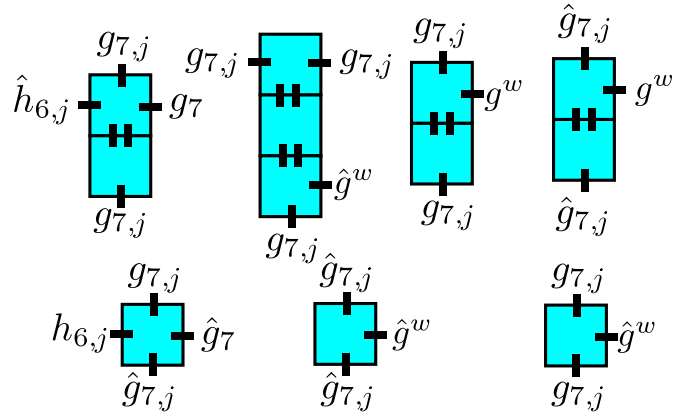


Fig. 39: The tiles and supertiles that bind to the west side of C_7^s for $s \geq 2$.

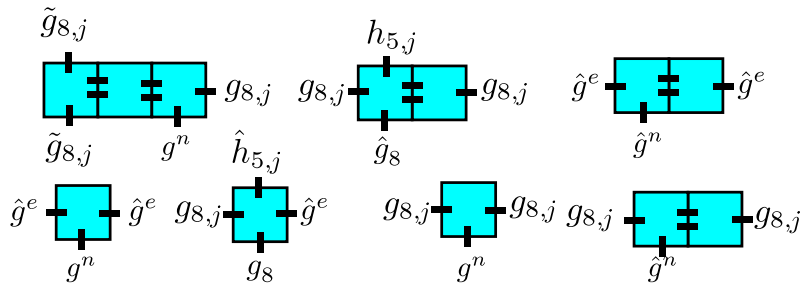


Fig. 40: The tiles and supertiles that bind to the north side of C_8^s for $s \geq 2$.

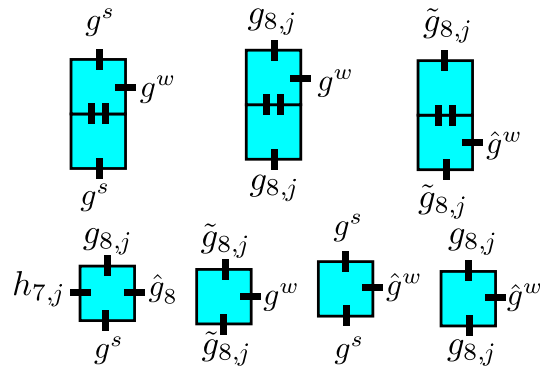


Fig. 41: The tiles and supertiles that bind to the west side of C_8^s for $s \geq 2$.